Available online at www.humg.edu.vn

ESASGD 2016

GIS–IDEAS (2016)

Conference Title: International Conference on GeoInformatics for Spatial-Infrastructure Development in Earth & Allied Sciences (GIS-IDEAS)

LONG-TERM CORRELATIONS BETWEEN SEA SURFACE HEIGHT AND SEA SURFACE TEMPERATURE IN THE EAST SEA

Võ Duy Long, Thái Tiểu Minh, Hồ Đình Duẩn*

Ho Chi Minh City Institute of Physics - Vietnam Academy of Science and Technology

Abstract

The correlation of Sea Surface Height (SSH) and Sea Surface Temperature (SST) in the East Sea is examined. This study uses Empirical Orthogonal Function(EOF) analysis individually and jointly on the two fields to determine spatial and temporal variation mode of SSH and SST then identify their principal modes of variation in East Sea. Thereby, the study defines the correlations between the modes of variation of SSH and SST in the East Sea. The ENSO index (NINO4) is also used to indicate the correlations of SSH and SST with the interannual variability. The spatial patterns of the EOF analysis show the regions in East Sea where there are large fluctuations of SSH and SST. The analyses of the temporal modes specify principal forms of the temporal fluctuations of SSH and SST. These modes of fluctuations present seasonal variation. By comparing the correlations of SSH and SST to ENSO index (NINO4), the correlation between mode 1 of the temporal components of SSH and NINO4 index is 0.67, the correlation between mode 3 of temporal components of SST and NINO4 index is 0.42, the results reveal the domination of ENSO in variations of SSH and SST in the East Sea. Another result in this study presents the spatial modes of the SSH and the SST, when their temporal modes co-vary in the same time period by using EEOF (Extend Empirical Orthogonal Functions) analysis.

Keywords: sea surface height, sea surface temperature, EOF analysis

1. Introduction

The atmospheric-oceanic interaction system is the result of complex interactions between many degrees of freedom, usually called modes. In order to offer visualization of atmospheric and oceanic processes, investigations about correlations of these parameters are necessary. One of the parameters of ocean is sea surface height (SSH), that displays variability of the surface of ocean and is affected by tidal forces, ocean circulation and variations in the gravitational field. The SSH is the deviation of the vertical position of the sea surface relative to a known reference surface. Ideally, this reference surface is the oceanic Geoid, but in practice it is commonly the mean of the SSH variations relative to an arbitrary reference ellipsoid computed during a specified time period. Another parameter is sea surface temperature (SST),it represents the temperature of ocean surface and plays a key role in regulating climate and variability of atmosphere. SSH and SST are the most fundamental parameters in ocean circulation and climate, their relationship provides information about the interaction between ocean and climate. There are many approaches about the correlations of parameters of ocean and climate including SSH, SST, sea level pressure, and wind stress, etc. Those researches present the

* Corresponding author. Tel.: +0-000-000-0000
E-mail address: duanhd@gmail.com.

correlations of parameters are different in regions and time scales Venegas, R. et al (2008). There are not many researches which present correlation of parameters of ocean and climate in regions of the East Sea.

In recent years, satellite data becomes common and it is used to analyze variability of parameters in many researches. Satellites have supplied data of SSH and SST and create convenient for investigating variability of ocean and climate in long timescale. The East Sea is a semi – enclosed basin in the western Pacific Ocean. There are many researches using satellite data to analyze variability of parameters in the East Sea. Chu et al (1997) used the National Center for Environment Prediction (NCEP) monthly SST data from 1982 to 1994 to study temporal and spatial variability. Seasonal variability of the SCS surface height have been reported in a number of investigations using satellite altimeter data of Ho et al (2000), Hwang and Chen (2000). Fang et al (2002) indicated trends and interannual variability of sea surface wind, SSH, SST in the East Sea by analyzing satellite data. However, these studies used data of short temporal interval and not represent correlation of SSH and SST variability in the East Sea.

The purpose of our study is to examine quantitatively correlations between ocean dynamics and climate variability in the East Sea. The region of our study extends from the Karimata Strait (4.5^0S) to the north of the Taiwan Strait (29.5^0N) and from the Andaman Sea (95.50^0E) to the Philippines Sea (136.5^0E). The main of the region is in the tropical Pacific where is controlled by El Niño Southern Oscillation (ENSO). ENSO is the largest source of interannual variability for the tropical Pacific, and it affects sea surface temperature, atmospheric pressure gradients, surface winds, ocean currents, thermocline depth, and biological productivity. NINO4 index (the ENSO indicator) shows the average sea surface temperature anomaly in the eastern equatorial Pacific (160^0E – 150^0W, 5^0S – 5^0N). Present study used NINO4 index to compare to fluctuation modes of SSH and SST. Empirical orthogonal functions (EOF) are used to analyze statistically the temporal and spatial variability of SSH and SST in the East Sea. Individual EOF analyses are made for SSH and SST data and joint EOF (EEOF) analysis is made on both parameters for the time period between October 1992 and December 2010.

2. Data and methods.

- SSH and SST Data

The data used in the present study is monthly mean SSH, SST data from October 1992 through December 2010. SSH anomaly data from AVISO (French space agency data provider) measured by several satellites including Envisat, TOPEX/Poseidon, Jason-1 and OSTM/Jason-2. This AVISO dataset was created by binning and averaging monthly values on 1 degree grids. Historical SST data have played an important role in researching long-term climate change. Owing to the importance of SST in climate variability, the variety of global gridded SST datasets has been independently created through historical ‘‘reconstruction’’ techniques, including the Optimum Interpolation SST (OISST), the Hadley Centre SST (HadSST), Extended Reconstructed SST (ERSST), Kaplan SST, and Centennial Observation Based Estimates of SSTs (COBE-SST). These datasets are based on in situ and satellite observations. The SST dataset was used in this study derived from monthly 1 degree gridded dataset Centennial Observation-Based Estimates of SST version 2 (COBE-SST2).For comparison, the data of SSH and SST are normalized. The normalized formula with the minimum and maximum value of SSH and SST are showed in (1) and Table 1, respectively.

$$X_{norm} = \frac{X - X_{\min}}{X_{mean}} - 1 \quad (1)$$

$$X_{mean} = \frac{X_{\max} - X_{\min}}{2} \quad (2)$$

Where, Xnorm is normalized data, X is original data, Xmin is minimum value of data, Xmax is maximum value of data.

Table 1. Maximum and minimum values of SSH and SST

	Max	Min
SSH (m)	1.8827	0.4906
SST (0C)	30.3	16.795

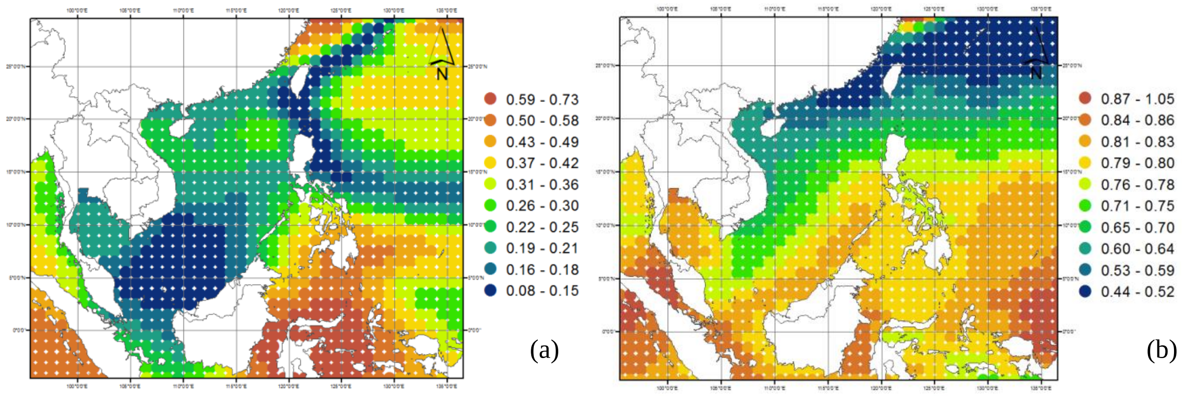

Fig. 1. RMS variability for SSH (a) and SST (b) for the period from October 1992 through December 2010

To show the regions where SSH and SST have the large variation, their root-mean-square (RMS) variabilities are displayed in Figure 1.The RMS variability is the square root of the temporal average of the squared variable at each grid point. In the Figure 1, the SSH variability is higher than 0.4 in the Celebes Sea and lower than 0.2 in total the East Sea of Vietnam. The SSH variability is lowest in the southern region of the East Sea of Vietnam and along the Taiwan Strait. The SST variability is higher than 0.78 in the southern and lower than 0.5 in the northern of the East Sea.

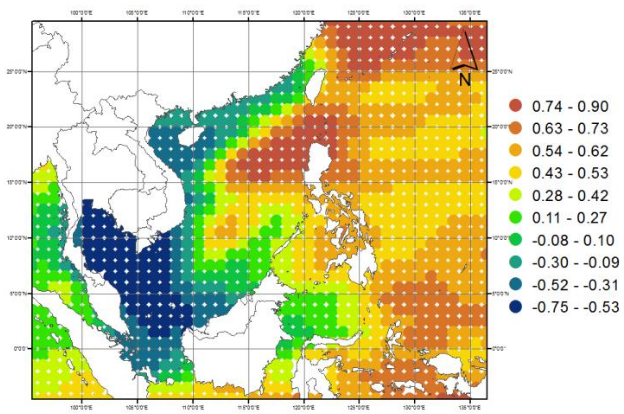

Fig. 2. Correlations map between SSH and SST

To present the co-variability between SSH and SST, correlations between the two time series are determined and their spatial distribution is shown in the Figure 2. The correlation map presents the correlation between SSH and SST in our study region, the positive correlations ($r > 0.4$) occur in the eastern of the East Sea, the negative correlations ($r < -0.5$) occur in the southern of the East Sea of Vietnam where extend from Gulf of Thailand to the Strait of Malacca.

- Method

The RMS variabilities and the correlation map present the spatial variability and co-variability of SSH and SST but they cannot indicate their temporal variability. In order to examine simultaneously their spatial and temporal variability, EOF analysis is implemented. In our research, EOF analysis are used to describe the spatial – temporal variability of the SSH and SST. The EOF modes are an efficient tool to present the main spatial – temporal variability of a dataset.

3. EOF Analysis.

EOF have been used in atmospheric science since the late 1940’s by Obukhov (1947, 1960), Fukuoka (1951), Lorenz (1956). Since then EOF become popular analysis tool and are use in the climate researches widely. Recently, EOF approaches are used to extract individual modes of variability that can be physically relevant such as the Arctic Oscillation (AO), (Pavan et al., 2000). The original intention of EOF (Obukhov 1947, 1960, Fukuoka 1951, Lorenz 1956) was to achieve a decomposition of a continuous space – time field X(t,s), where t and s denote respectively time and spatial position, as

$$X(t,s) = \sum_{k=1}^{m} c_k(t) u_k(s) \quad (3)$$

Where, *m* is the number of modes contained in the field, are the principal (temporal) components of the spatial components .The principal and spatial components are calculated from the eigenvectors and eigenvalues of the m x m spatial covariance matrix of the data set. A matrix X of the spatial anomalies can be constructed with m sampling locations and n sampling times.

$$X = \begin{bmatrix} X_{11} & X_{12} & \cdots & X_{1n} \\ X_{21} & X_{22} & & \vdots \\ \vdots & & \ddots & \vdots \\ X_{m1} & \cdots & \cdots & X_{mn} \end{bmatrix} \quad (4)$$

Covariance matrix V can be found

$$V = \frac{1}{m} X^T X \quad (5)$$

Where the superscript ‘T’ indicates the matrix transpose. The eigenvectors and eigenvalues of V satisfy the equation

$$VE = EL \quad (6)$$

Where E is a n x n matrix contains the eigenvectors as columns, L is a n x n matrix that contains the associated eigenvalues along the diagonal. The eigenvalues are contained in L that represent the variances. The total variance of the spatial anomaly data is invariant is the sum of the diagonal values E is also called as the matrix of EOF pattern. Figure 3 show percentages of the explained variance associate with each component of SSH and SST.

EEOF are calculated from the covariance matrix constructed from both variables show the area where both variables co-vary tightly. Applies this method two different fields X and Y. From the cross – covariance matrix $C = X.Y^T$, the matrix C is used to analyze EOF of the two fields.

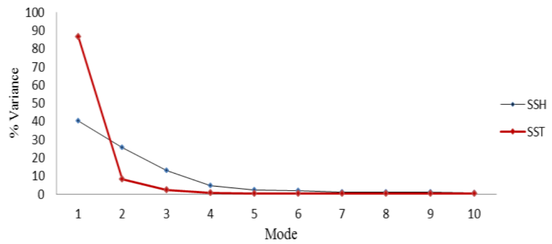

Fig. 3. Correlations map between SSH and SST

3.1. EOF for SSH and SST

Figure 4 shows the spatial distributions and the principal (temporal) components for mode 1, which account for 40.2% and 86.3% of the total variance for SSH and SST, respectively. The patterns of the high SSH values occur in the southern of the East Sea of Vietnam, the low SSH values occur in the Philippines Sea in the interval time from October 1992 to May 1998 and in the interval time from December 2001 to April 2005, when the SSH principal components (blue line in Figure 4c) are positive. When the SSH principal component (blue line in Figure 4c) is negative, the patterns of SSH switch from low SSH values in the southern of the East Sea of Vietnam to high SSH values in the Philippines Sea in the interval time from June 1998 to November2001 and in the interval time from April 2007 to November 2009.The NINO 4 index (red line in Figure 4c) is showed to compared to fluctuation modes of SSH and SST.

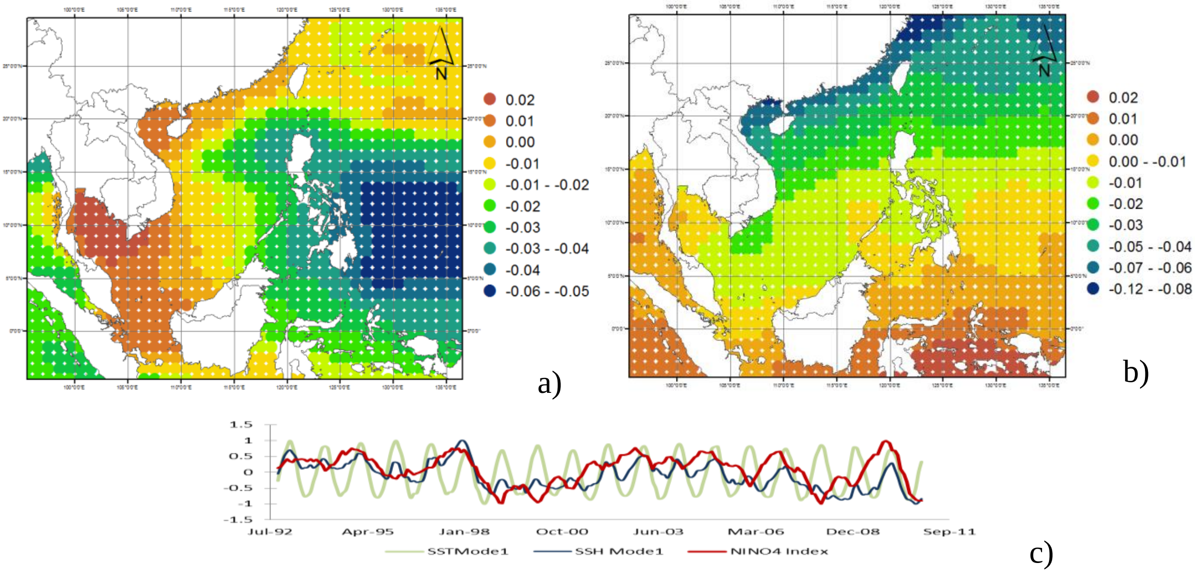

Fig. 4. Spatial patterns for mode 1 of the individual EOF analyses of a) SSH b) SST, and c) the normalized principal components for SSH and SST

The correlation between NINO 4 index with the SSH principal component is 0.67 (Table 2).Moreover, the first SST principal component presents distinctly seasonal variation. Figure 4c shows the interannual variations of SSH and NINO4 index. The SSH values indicate seasonal variation in the East Sea. Figure 5 shows the spatial distributions and the principal components for mode 2, which account for 25.4% and 8.3% of the total variance for SSH and SST, respectively. The patterns of SSH fluctuation are high in Gulf of Thailand and low in Bashi Strait. However, the patterns of SST fluctuation are high in the southern of the East Sea of Vietnam of and low in the north of the Taiwan Strait. These fluctuations switch according to seasonal cycle. The SST principal components of mode 1 have the correlation with the SSH principal components of mode 2 which is -0.68 (Table 2). The SSH and SST spatial components of mode 2 have correlation with the SSH and SST spatial component of mode 1 that is -0.63 (Table 3).

Figure 5 shows the spatial distributions and principal components for mode 3, which accounts for 12.7% and 2.3% of the total variance for the SSH and the SST, respectively. Correlations between the spatial and principal components of the SSH and the EOF analyses of the SST are given in Table 1 and Table 2.

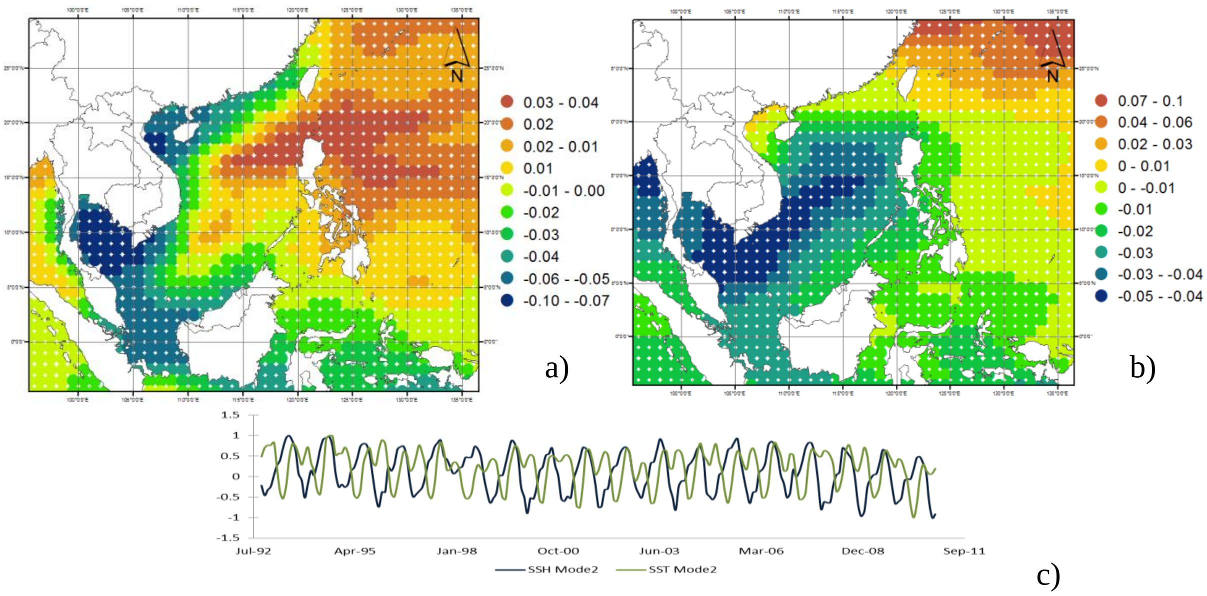

Fig. 5. Spatial patterns for mode 2 of the individual EOF analyses of a) SSH b) SST, and c) the normalized principal components for SSH and SST

The mode 1 spatial components for SST and mode 3 spatial components for SSH have the high correlation (r = 0.82), their principal components have the correlation, which is 0.54.The correlations of the mode 1 of SSH and the mode 3 of SST in the spatial and principal components are 0.56 and 0.42, respectively. The trend line of the mode 3 of SST in the principal components also shows the interannual variation resemble the mode 1 of SSH in the principal components (Figure 9).

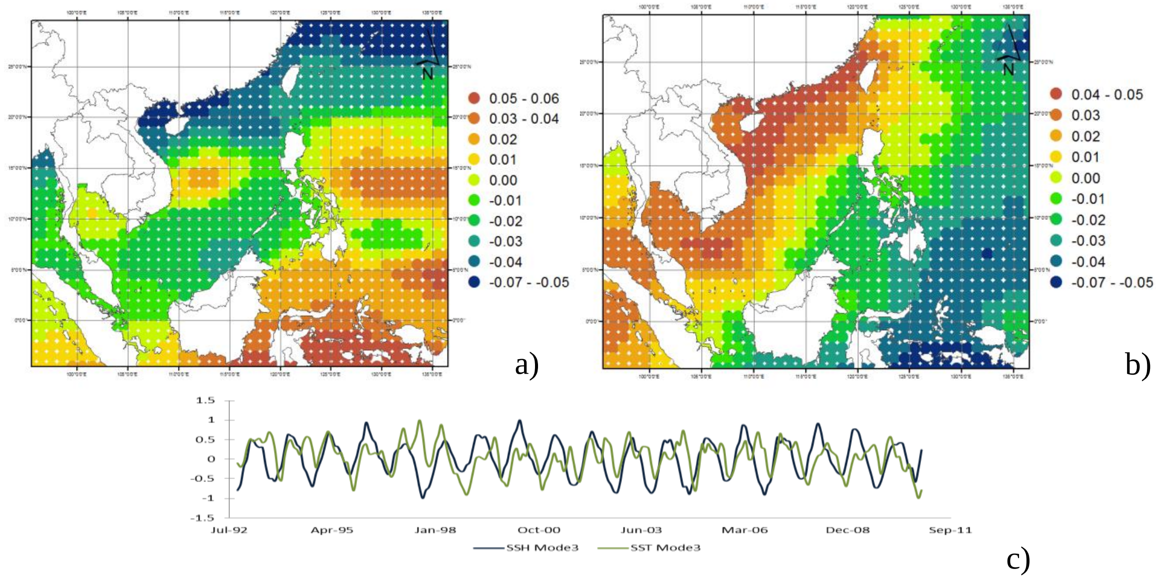

Fig. 6. Spatial patterns for mode 3 of the individual EOF analyses of a) SSH b) SST, and c) the normalized principal components for SSH and SST

3.2. EEOF for SSH and SST

EEOF (Extend Empirical Orthogonal Functions) are calculated from the covariance matrix constructed from joint variables (in our case that is SSH values and SST values) to highlight how they co-vary with each other, forcing them to have the same temporal variability but different patterns of spatial variability (Wilson and Adamec, 2001). The first mode of the joint analysis is accounted for 95.6% of the total variance. Its spatial and principal components are showed in Figure 7. The spatial components of the individual and joint analyses are correlated from -0.61 to -1 for SSH and SST, respectively, and from -0.68 to -1 for the principal components (Table 1 and Table 2). In the spatial components of mode 1, the high SSH values are concentrated in the eastern and northern and the low SSH values are concentrated in the southern of the East Sea of Vietnam. These concentrations resemble the concentrations of the correlation of SSH and SST in Figure 2.

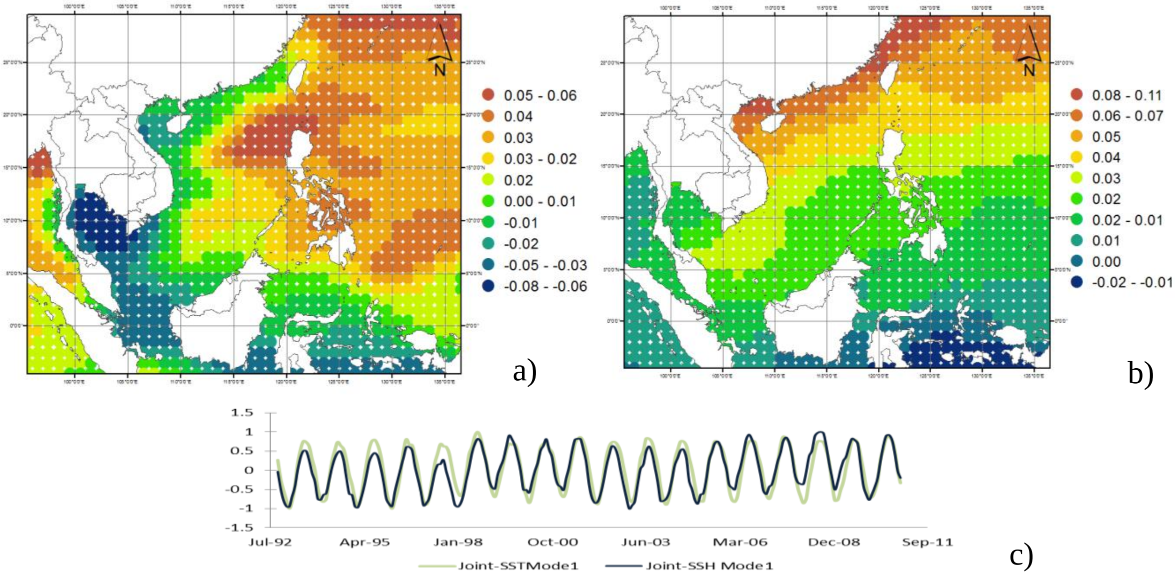

Fig. 7. Spatial patterns for mode 1 of the joint EOF analyses of a) SSH b) SST, and c) the normalized principal components for SSH and SST

The high SST values focus in northern and decrease quickly in southern. The correlation between joint spatial SSH mode 1 and joint spatial of SSH mode 2 is 0.95. The second mode of the joint analysis accounts for 2.3% of the total variance. Its spatial and principal components are showed in Figure 8.

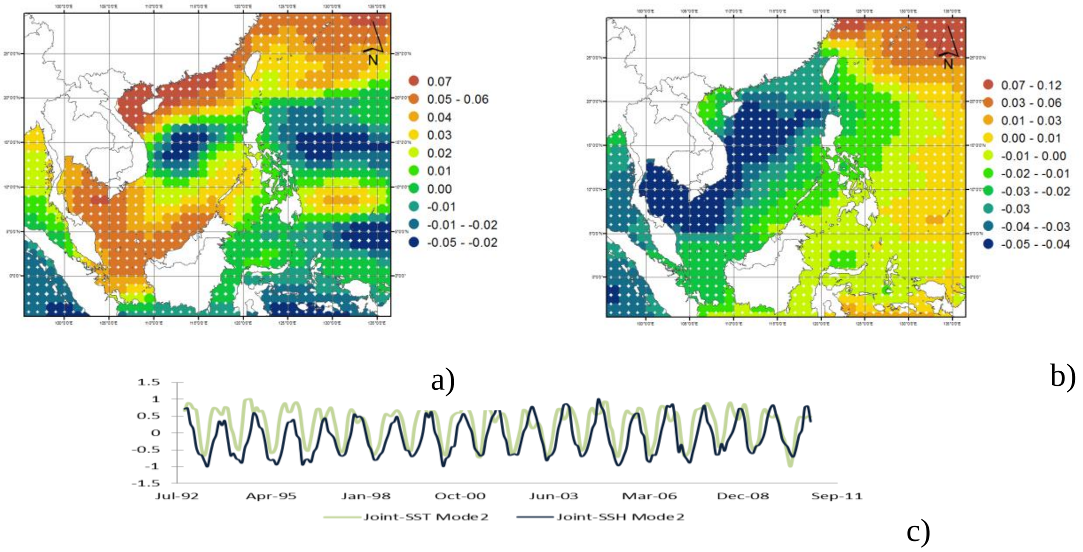

Fig. 8. Spatial patterns for mode 2 of the joint EOF analyses of a) SSH b) SST, and c) the normalized principal components for SSH and SST

The spatial components in the EOF and EEOF analyses are correlated at 0.89 for SST, and at 0.96 for the principal components (Table 1 and Table 2). Spatial distributions of the joint spatial components of the SSH values and the SST values in mode 2 are quite opposite. The high SSH values are mostly concentrated in the East Sea of Vietnam, however the SST values are contrary. EEOF analysis shows the spatial modes of the SSH and the SST when their temporal modes co-vary in the same time period.

4. Conclusions and discussion.

Table 2. Correlation coefficients between principal components from SSH and SST of EOF and EEOF analyses (individual and joint) and NINO4 index.

	SSH M1	SST M1	SSH M2	SST M2	SSH M3	SST M3	J-SSH M1	J-SST M1	J-SSH M2	J-SST M2	NINO4
SSH M1	1.00										
SST M1	0.43	1.00									
SSH M2	0.00	-0.68	1.00								
SST M2	0.14	0.00	-0.15	1.00							
SSH M3	0.00	0.54	0.00	-0.50	1.00						
SST M3	0.42	0.00	0.59	0.00	0.25	1.00					
J-SSH M1	-0.68	-0.90	0.68	-0.08	-0.27	0.04	1.00				
J-SSTM1	-0.43	-1.00	0.68	-0.01	-0.53	0.00	0.91	1.00			
J-SSH M2	-0.04	-0.01	-0.61	0.55	-0.78	-0.55	-0.18	0.00	1.00		
J-SST M2	-0.01	-0.10	-0.24	0.96	-0.62	-0.27	0.00	0.10	0.69	1.00	
NINO4	0.67	-0.08	0.26	0.06	-0.35	0.41	-0.18	0.08	0.07	-0.02	1.00

The present study shows the principal modes of variations of the SSH and the SST in the East Sea. The analysis results present the SCS regions where there are large fluctuations of the SSH and the SST. The main spatial modes of the variation of the SSH indicate strong variation in Gulf of Thailand and the Philippines Sea, they are accounted for 65.6% of the total variance. The main spatial modes of variation of the SST present the regions where large variation appears. Mode 1 that is accounted for 86.3% of the total variance presents large variation of the main of the region in the Northern and Southern areas. Mode 2 is accounted for 8.3% of the total variance and present large variation in the East Sea of Vietnam and the Philippines Sea. The analyses of the temporal modes specify the principal forms of the temporal fluctuations of the SSH and the SST. The modes of fluctuations present seasonal variation. The variations of SST in seasonal is not surprisingly because temperature is varied in seasonal. It is remarkable that the SSH also varies in seasonal. It indicates that temperature affect to fluctuation of sea surface. The correlations of the SSH and the SST in temporal and spatial are summarized in Table 1 and Table2, it indicate there are correlations of modes of SSH and SST. Correlation coefficients between mode 1 of spatial component of SST and mode 2 of spatial component of SSH in EOF is 0.82.The study also analyses the modes for interannual variation by comparing the correlation of SSH and SST to ENSO index (NINO4). The correlation between mode 1 of temporal component of SSH and NINO4 index is 0.67 and the correlation between mode 3 of temporal component of SST and NINO4 index is 0.42.

Table 3. Correlation coefficients between spatial components from SSH and SST of EOF and EEOF analyses (individual and joint) and NINO4 index.

	SSH M1	SST M1	SSH M2	SST M2	SSH M3	SST M3	J-SSH M1	J-SST M1	J-SSH M2	J-SST M2
SSH M1	1.00									
SST M1	-0.31	1.00								
SSH M2	-0.63	-0.23	1.00							
SST M2	-0.10	-0.63	0.44	1.00						
SSH M3	-0.40	0.82	-0.12	-0.39	1.00					
SST M3	0.56	-0.40	-0.30	-0.29	-0.55	1.00				
J-SSH M1	-0.61	-0.36	0.95	0.48	-0.35	-0.16	1.00			
J-SSTM1	0.30	-1.00	0.23	0.61	-0.82	0.43	0.36	1.00		
J-SSH M2	0.60	-0.65	-0.35	0.25	-0.83	0.47	-0.13	0.64	1.00	
J-SST M2	-0.24	-0.32	0.40	0.89	-0.09	-0.66	0.37	0.29	0.06	1.00

Our results reveal that mode 1 of temporal component of SSH and mode 3 of temporal component of SST are controlled by interannual variation and they are showed in Figure 9.The ENSO events dominate variation of SSH and SST in the East Sea. Our study also shows the spatial modes of the SSH and the SST when their temporal modes co-vary in the same period by using EEOF analysis.

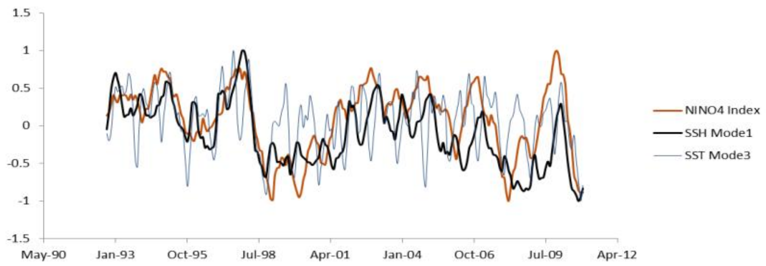

Fig. 9. Nomalized principal components for mode 1 of SSH and mode 3 of SST are compared with NINO4 index

The correlations of SSH and SST that the study presents are relatively low. In some cases, however, the coefficients of SSH and SST have a significant correlation. These correlations express interaction of SST and SSH, however it is still not enough base to assert that they affect directly together. The cause of these interaction that need more investigations and we will examine in future study..

Acknowledgements

We thank the NOAA/OAR/ESRL PSD, Boulder, Colorado, USA who provided sea surface temperature data. We thank AVISO who provided sea surface height data in our study. Additional thanks are directed to the reviewers who gave valuable comments on an first draft of the manuscript.

References

Chu, P. C., S. Lu, and Y. Chen., 1997. Temporal and spatial variabilities of the South China Sea surface temperature anomaly, J. Geophys. Res. , 102(C9), 20,937– 20,955.

Fang, W., G. Fang, P. Shi, Q. Huang, and Q. Xie., 2002. Seasonal structures of upper-layer circulation in the southern South China Sea from in situ observations, J. Geophys. Res. , 107(C11), 3202.

Fukuoka, A., 1951. A study of 10-day forecast (A synthetic report). The Geophysical Magazine, Tokyo, Vol. XXII, 177-218.

Ho, C.-R., Q. Zheng, Y. S. Soong, N.-J. Kuo, and J.-H. Hu., 2000. Seasonal variability of sea surface height in the South China Sea observed with TOPEX/Poseidon altimeter data, J. Geophys. Res. , 105(C6), 13,981– 13,990.

Hwang, C., and S.-A. Chen., 2000. Circulation and eddies over the South China Sea derived from TOPEX/Poseidon altimetry, J. Geophys. Res., 105(C10), 23,943–23,965.

Lorenz, E. N., 1956. Empirical orthogonal functions and statistical weather prediction. Technical report, Statistical Forecast Project Report 1, Dept. of Meteor., MIT, 1956. 49pp.

Pavan V., Tibaldi S, Brankovich C., 2000. Seasonal prediction of blocking frequency: results from winter ensemble experiments. Quarterly Journal of the Royal Meteorological Society 126: 2125–2142.

Obukhov, A.M., 1947. Statistically homogeneous fields on a sphere. Usp. Mat. Navk., 2, 196-198.

Obukhov, A. M., 1960. The statistically orthogonal expansion of empirical functions. Bull. Acad. Sci. USSR Geophys. Ser. (English Transl.), 288-291.

Venegas, R., P.T. Strub, E. Beier, R. Letelier, A.C. Thomas, T.Cowles, C. James, L. Soto-Mardones, C. Cabrera., 2008. Satellite-derived variability in chlorophyll, wind stress, sea surface height, and temperature in the northern California Current System, J. Geophys. Res., v.113, 2008.

Wilson, C. and Adamec, D., 2001. Correlation between chlorophyll and sea surface height in the tropical Pacific during 1997–1999 El Niño Southern Oscillation event, J. Geophys. Res., 106, 31175 – 31188.